Full article
doi.org/10.1002/elsa.202100059
Chemistry Europe
European Chemical Societies Publishing

Received: 1 April 2021
Revised: 1 May 2021
Accepted: 2 May 2021

Corrosion inhibition effect of *Cycas revoluta* leaves extract on corrosion of soft-cast steel in hydrochloric acid medium

Manohar R. Rathod | **S. K. Rajappa**

Department of Chemistry, Karnatak Science College, Dharwad, India

Correspondence
Dr. S. K. Rajappa, Department of Chemistry, Karnatak Science College, Dharwad 580001, India.
Email: drrajappask@gmail.com

Abstract

The inhibition action of environmentally sustainable inhibitor *Cycas revoluta* leaves extract *(CRLE)* for corrosion protection of soft-cast steel in a solution of HCl was assessed with electrochemical and chemical methods. The eco-friendly inhibitor forms a thin coating on soft-cast steel and slows the corrosion in acid media. The percent inhibition performance, corrosion current density, corrosion potential, and both anodic and cathodic slopes for Tafel were calculated. The results for electrochemical and chemical research are in beneficial correlation with each other. The inhibitor's inhibitory ability was well illustrated by the *CRLE* adsorption on soft-cast steel followed the Langmuir isotherm. The investigations reveal that *CRLE* is a mixed form of inhibitor. Studies were performed with varying inhibitor amounts and temperatures. Thermodynamic parameters were calculated, and it shows that the corrosion inhibition effect is spontaneous and exothermic. The interaction of the plant extract was characterized by SEM, FTIR, contact angle measurements, and AFM techniques.

KEYWORDS
CRLE, *EIS*, inhibitor, soft-cast steel, Tafel

1 | INTRODUCTION

Soft-cast steel is commonly used for mass production for its cheap rate, mechanical strength, and deformability, and plenty of other features.[1] Industries heavily depend on the metal and their alloys, and during this process, they are exposed to corrosive media to form a stable compound and during this process mass loss of the metal occurs, and the external metal surface corrodes and termed as corrosion. Acid treatments for industrial applications are also used, for example, chemical cleaning, pickling, industrial processing, de-scaling, acidizing, and so on.[2-6] Corrosion is a big problem to society that causes economic loss in the industrial sector because lot of investment is made annually on corrosion-related issues.[7,8] Several methods such as cathodic protection, application of the coating, and corrosion inhibitors are employed to overcome this problem by reducing the rate of corrosion of metals and their alloys.[9–14] The extracts of plants are considered as an efficacious inhibitor for corrosion including *Tagetes erecta*,[15] *Pimenta dioica*,[16] *Azadirachta indica* extract,[17] and *Justicia gendarussa* plant extract[18] have briefed as to the finest inhibitor for corrosion in the corrosive medium. The medicinal plant *Cycas revoluta* was included in this research because its leaves yielded 12 components, seven of which were identified over the first occasion for this genus. Fourteen biflavonoids, three lignans, three flavan-3-ols, two flavone-C-glucosides, two nor-isoprenoids, and

Abbreviations: CRLE, *Cycas revoluta* leaves extract

This is an open access article under the terms of the Creative Commons Attribution License, which permits use, distribution and reproduction in any medium, provided the original work is properly cited.
© 2021 The Authors. *Electrochemical Science Advances* published by Wiley-VCH GmbH

Full article
doi.org/10.1002/elsa.202100059
Chemistry Europe
European Chemical Societies Publishing

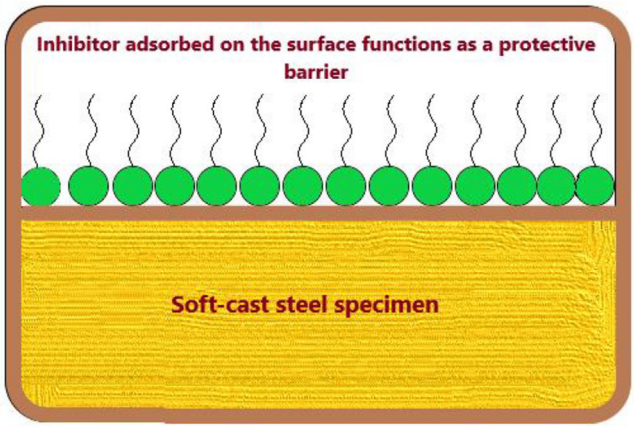


FIGURE 1 Represents the adsorption of inhibitor molecules on soft-cast steel

one flavanone were extracted from the species.[19] The whole plant seems to have a wide variety of applications, including food preparation, household products, traditional medicine, pharmacognosy, and diagnosis of gastric cancer cell formation, migration, and invasion.[20] Specifically, the leaves of this plant exhibit antimicrobial and antioxidant properties.[21] These phytochemicals present in the plant bind to the soft-cast steel and form a thin coating, slowing down corrosion in hydrochloric acid shown in Figure 1. The green inhibitor derived from the plant source is closer to the chemical composition of traditional organic corrosion inhibitors.

The present work is carried out for the plant extract obtained from the leaves of *Cycas revoluta* and further was subjected to corrosion-protection studies for soft-cast steel in hydrochloric acid.

2 | MATERIALS AND METHODS

2.1 | Inhibitor preparation

The leaves of *Cycas revoluta* were taken from the botanical garden of Karnatak Science College, Dharwad, India, and washed under running water. The leaves were dried in the sunlight for 6 days and ground to a powder with a mechanical grinder. Soxhlet extraction is an efficient method to extract useful active molecules from a wide range of natural materials. In this work, 30 g of powdered leaves and 300 mL of ethanol were taken in soxhlet apparatus over the period of 5 h for extraction process. The extract containing an excess of ethanol was expelled by a rotary evaporator, and obtained 4.7 g of the solid residue, and the complete solid sample was used to prepare the stock solution, therefore it was taken in the range of 0.47, 0.94, 1.41, and 1.88 g/L.

2.2 | Preparation of test solutions

HCl (1 M) and *CRLE* test solution for varying concentrations are prepared for corrosion studies with analytical-grade chemicals and double-distilled water.

2.3 | Sample preparation

For corrosion studies, commercial-grade soft-cast steel with composition (Mn 0.5%, C 0.19%, P 0.05%, S 0.04%, Si 0.2%, and remainder Fe 99.02%) sheets with 0.1 cm thickness were selected. For mass-loss measurements, rectangular plates with exposed areas of $5 \times 1 \times 0.1$ cm are being utilized, and soft-cast steel used as a working electrode with a surface area of 1 cm^2 was exposed for electrochemical measurements, while the remaining portion was coated with chemical-resistant epoxy coating. Soft-cast steel was glazed by sandpaper of different grades (180-2000) until a mirror finish was achieved, beginning with the coarsest to the fine grade. The specimens were cleaned properly with doubly distilled water, dried, and stored in a desiccator before testing.

2.4 | Mass-loss measurements

To evaluate the rate of corrosion and inhibition effect of soft-cast steel in the hydrochloric acid, mass-loss experiments were performed. Using electronic digital balance *(Scale Tech)*, the washed & dry specimens were weighed and suspended in a 100 mL beaker containing acid or acid solution with differing inhibitor concentrations and placed in a thermostat. The specimens were removed after the specified immersion time, washed in running water, cleaned, dried, and placed in a desiccator to reach room temperature and weighed. All the measurements were done twice, and the results were given as average mass-loss values.

2.5 | Electrochemical measurements

In the CHI608D (CH Instruments produced in Austin, United States) electrochemical workstation, electrochemical tests were carried out at 300 ± 1 K. Three electrodes consist of the membrane, specifically the working electrode (soft-cast steel), the auxiliary electrode, and the glass electrode (Ag/AgCl). To determine the open-circuit potential (OCP) of the test solution, the soft-cast steel electrode was allowed to stand in the test solution for 30 min before each electrochemical measurement. All the measured potentials were correlated with the Ag/AgCl electrode. The possible range acquired by adding –0.2 to +0.2 V

Full article
doi.org/10.1002/elsa.202100059
Chemistry Europe
European Chemical Societies Publishing

to a value of OCP, potential-current profiles were recorded at a scanning rate of 0.01 V/s for Tafel readings. The corrosion potential *(E_{corr})*, corrosion current *(I_{corr})* cathodic *(β_c)*, and anodic *(β_a)* Tafel slope corrosion variables were measured. Impedance assessments were carried out with an AC signal of 5 mV amplitude and an OCP frequency spectrum of 0.1 Hz to 1 kHz. The Z_{Simp} Win 3.21 application was used to match the impedance data to the most suitable equivalent circuit. The Nyquist plots are often used to acquire impedance parameters.

2.6 | Adsorption isotherm and thermodynamic considerations

Plant extract *(CRLE)* is an effective inhibitor that binds to the metal surface and protects soft-cast steel corrosion in acidic environments. Different parameters for adsorption were determined and analyzed. The adsorption of *CRLE* follows Langmuir adsorption isotherm. The activation parameter for soft-cast steel corrosion with and without *CRLE* components was examined through the mass-loss method for temperature 300±1 to 320 ±1K using standard equations.

2.7 | FT-IR spectroscopic studies

Using a Nicolet 5700 FT-IR spectrometer with a wavelength of 4000 to 400 cm^{-1} for *CRLE* extract, FT-IR spectra were recorded to specify the functional group and the correlation of these groups on the soft-cast steel surface during acidic corrosion.

2.8 | Surface characterization

The soft-cast steel surface morphologies were investigated by the approach of the scanning electron microscope (SEM: Model-JEOL make, JSM-IT 500LA), Atomic force microscopy (AFM-Nanosurf® EasyScan 2), and water contact angle (Model-DMs-401 famas software make: Kyowa interface science Co. Ltd Japan) techniques. The specimen was dipped in the test solution without and with *CRLE* for 2 h at ambient temperature to receive images of the working electrode.

3 | RESULTS AND DISCUSSION

3.1 | Mass-loss method

Table 1 represents the rate of corrosion and percentage inhibition performance of soft-cast steel with varying concentrations of *CRLE* in 1 M HCl at 300 ± 1 K. In the absence of an inhibitor, the rate of corrosion is greater due to the presence of a significant amount of H^+ ions in the acid medium, which hikes the rate of the reduction reaction.

Compared to the acidic media, *CRLE* reduces corrosion in soft-cast steel, and the inhibition performance *(η_w)* is enhanced with an increased concentration of inhibitor. The highest η_w 96.66 was recorded for *CRLE* at an optimized concentration of inhibitor for 1 M HCl solution. As the inhibitor concentration was raised, no significant rise in the η_w was observed, so 1.88 g/L was considered the optimum concentration of the inhibitor. The inhibitor concentration above 1.88 g/L may lead to the weakening of metal-inhibitor interactions, resulting in the replacement of inhibitor by water or chlorine ions with a decrease in inhibition efficiency. Further hydrogen evolution is also dominated in acidic solution. Hence, mass build-up is not taking place over the soft-cast steel surface. The *CRLE* molecules are protonated in an acid medium, and these protonated molecules lead to the decline in the reduction reaction. The addition of inhibitor components binds to the surface of soft-cast steel and develops a thin coating that segregates the surface of the metal from the acid media and controls soft-cast steel corrosion.[22]

3.2 | Potentiodynamic polarisation studies

The Tafel polarization plots without and with varying concentrations of *CRLE* in 1 M HCl for soft-cast steel at the range of temperature 300 ± 1 K are presented in Figure 2.

Corrosion variables such as corrosion potential *(E_{corr})*, corrosion current density *(i_{corr})*, rate of corrosion (υ), cathodic *(β_c)* and anodic *(β_a)* Tafel slope, and inhibition performance *(η_w)* were calculated by this approach have been recorded in Table 2. The inhibition performance $\%\eta_W$ of the *CRLE* for soft-cast steel was measured by the expression:

$$\%\ \eta_w = \frac{i^o_{corr} - i_{corr}}{i^o_{corr}} \times 100$$

where i_{corr} and i^o_{corr} are the corrosion current density without and with *CRLE* for soft-cast steel.

The outcomes of such measurement techniques (Figure 2 and Table 2) were interpreted as follows:

There is a slight improvement in the inhibited solution's corrosion potential *(E_{corr})* relative to an uninhibited solution that does not exceed 85 mV. These findings demonstrate that the *CRLE* inhibitor exhibits a mix-type inhibitor, decreasing both reactions of anodic metal dissipation and reaction of cathodic hydrogen liberation.[23,24]

Full article
doi.org/10.1002/elsa.202100059
Chemistry Europe
European Chemical Societies Publishing

TABLE 1 At 300 ± 1 K mass-loss criteria for soft-cast steel in 1 M HCl without and with various inhibitor concentrations

1 M HCl				
Time (hours)	**Concentration (g/L)**	**Corrosion rate (mpy)**	**Inhibition efficiency ($\%\eta_w$)**	**Surface coverage (θ)**
1	Blank	183.85		
	0.47	30.64	83.33	0.8333
	0.94	18.38	90	0.90
	1.41	12.25	93.33	0.9333
	1.88	6.12	96.66	0.9666
2	Blank	189.98		
	0.47	30.64	83.87	0.8387
	0.94	21.44	88.70	0.8870
	1.41	15.32	91.93	0.9193
	1.88	9.19	95.16	0.9516
3	Blank	196.10		
	0.47	28.59	85.41	0.8541
	0.94	22.47	88.54	0.8854
	1.41	16.34	91.66	0.9166
	1.88	10.21	94.79	0.9479
4	Blank	193.04		
	0.47	27.57	85.71	0.8571
	0.94	22.98	88.09	0.8809
	1.41	15.32	92.06	0.9206
	1.88	9.19	95.23	0.9523
5	Blank	205.91		
	0.47	31.86	84.52	0.8452
	0.94	23.28	88.69	0.8869
	1.41	15.93	92.26	0.9226
	1.88	11.03	95.23	0.9523

- There has been a substantial reduction in corrosion current density and corrosion rate (υ) of soft-cast steel by a rise in *CRLE* concentrations in 1 M HCl. Since inhibitor molecules adsorb to the surface of soft-cast steel, they prevent the corrosion sites on the surface from the bulk medium.
- Reducing values of i_{corr} of the inhibited solution compared to non-inhibited solution lead to a rise in inhibition of the inhibitor's efficiency for soft-cast steel in 1 M HCl. We noticed an improvement in η_w values with an increase in *CRLE* concentrations in 1 M HCl.
- The rise in η_w rises with a rise in the inhibitor concentration at a temperature range of 300±1K for soft-cast steel 1 M HCl. The highest inhibition performance was found to be 88.84% at 1.88 g/L of *CRLE* because of the adsorption of CRLE on a soft-cast steel surface.
- A slight shift in the movement of the cathodic (β_c) and anodic (β_a) Tafel slope has demonstrated that *CRLE* hinders the corrosion of soft-cast steel by adsorption without affecting the corrosion mechanism.

Test results of electrochemical polarization research have shown that *CRLE* is a propitious soft-cast steel corrosion resistor in 1 M HCl solution.

3.3 | Electrochemical impedance measurements

EIS calculations for soft-cast steel were performed without and with varying concentrations of *CRLE* in 1 M HCl at a range of temperature 300 ± 1 K. As shown in Figure 3, the EIS spectrum was measured, and the computed corrosion parameters, viz., resistance polarization (R_p), double-layer capacitance (C_{dl}), and inhibition performance (η_w) were recorded by the proper equivalent circuit as presented in Figure 4 and have been included in Table 3. The inhibition

Full article
doi.org/10.1002/elsa.202100059
Chemistry Europe
European Chemical Societies Publishing

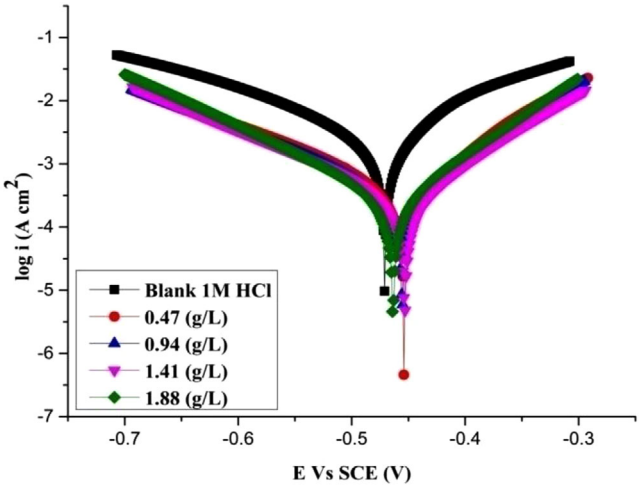


FIGURE 2 For 1 M HCl at 300 ± 1 K polarization curves for soft-cast steel in the absence and presence of *CRLE*

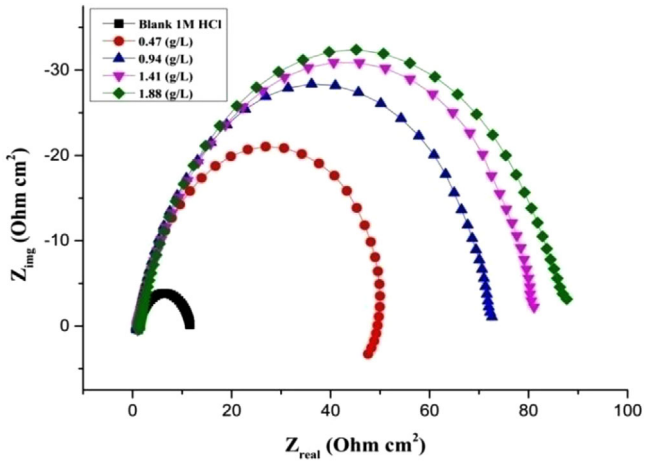


FIGURE 3 Soft-cast steel Nyquist plots in 1 M HCl in the absence and presence of varying concentrations of *CRLE*extract at 300 ± 1 K

performance of soft-cast steel in 1 M HCl with varied concentrations of inhibitor by using the following relation

$$\% \eta_w = \frac{R_{P(inh)} - R_{P(0)}}{R_{P(inh)}} \times 100$$

where $R_{P(inh)}$ and $R_{P(0)}$ are represented as the values of polarisation resistance of inhibited and uninhibited solution. Double-layer capacitance (C_{dl}) values were computed using the equation:

$$C_{dl} = (QR_{ct}^{1-n})^{1/n}$$

The constant phase factor (CPE) is Q and n is the exponent of CPE, which gives descriptions of the degree of homogeneity of the surface. There is a set of semicircles in the EIS spectrum (Nyquist plots) with high frequencies capacitive loop and a reduced inductance circuit. The following investigation was conducted on the effects of the EIS measurements recorded in Table 3.

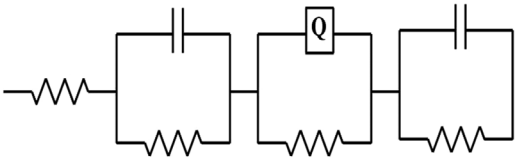


FIGURE 4 Equivalent circuit fit for the Nyquist graphs of *CRLE*

TABLE 2 Corrosion measurements for soft-cast steel achieved using the polarization method in 1 M HCl at 300 ±1K

Conc. of Acid (M)	Concentration (g/L)	-E $_{corr}$(V vs SCE)	I$_{corr}$ (A cm^{-2})	β a(V/dec)	β c(V/dec)	C.R. (mil/yr)	(%η_W)
1 M	Blank	-0.400	2.515×10^{-3}	6.776	7.512	1.484×10^{-3}	—
	0.47	-0.454	3.556×10^{-4}	12.130	7.361	2.037×10^{-2}	85.86
	0.94	-0.456	3.044×10^{-4}	12.059	7.384	1.770×10^{-2}	87.89
	1.41	-0.453	2.827×10^{-4}	11.476	7.549	1.643×10^{-2}	88.75
	1.88	-0.464	2.806×10^{-4}	12.216	8.615	1.631×10^{-2}	88.84

TABLE 3 Corrosion parameters for soft-cast steel achieved using the EIS approach in 1 M HCl at 300±1K

Conc. of acid (M)	Concentration (g/L)	R$_p$ (Ω cm^2)	C$_{dl}$ (μF/cm^{-2})	(%η_W)	Surface coverage (θ)
1 M	Blank	8.392	2463	—-	
	0.47	41.70	1431	79.88	0.7988
	0.94	66.01	818	87.28	0.8728
	1.41	76.11	232	88.97	0.8897
	1.88	77.47	141	89.16	0.8916

Full article
doi.org/10.1002/elsa.202100059
Chemistry Europe
European Chemical Societies Publishing

- In the Nyquist plot, the value of R_p is defined as the diameter of the semicircle. As metal dissolution is controlled, the diameter or R_p values of inhibited solution hike with rising *CRLE* concentrations. The inhibitor binding is attributed to the surface coverage of soft-cast steel in the 1 M HCl.
- The rise in double-layer thickness because of the formation of a protective coat on the metal/solution interface slows down the corrosion process. The double-layer capacitor (C_{dl}) values decline with a rise in *CRLE* concentration.[25]
- The inhibition performance increases with a rise in the concentration of *CRLE* to the acid media. This is due to strong inhibitor adsorption, which controls the desorption mechanism of the metal surface.[26] At an optimized concentration of 1.88 g/L of *CRLE* at 300±1K, we identified a peak inhibition efficiency of 89.16%.

The EIS calculation reveals the *CRLE* serves as a propitious inhibitor for corrosion of soft-cast steel in 1 M HCl. The results reported in the EIS measurements are similar to the findings indicated in the measurements of potentiodynamic polarization.

3.4 | Activation parameters

The impact of temperature on an inhibited soft-cast steel surface with the acidic medium is highly volatile, as numerous modifications generally occur on the surface layer, include etching, inhibitor desorption, decomposition, and rearrangement.[27] The impact of temperature on the corrosion rate of soft-cast steel in 1 M HCl solution in the existence of varied concentrations of *CRLE* was examined at temperatures ranging from 300 ± 1 to 320 ± 1 K as presented in Table 4. The corrosion rate rises both without inhibitor and rise in temperature for soft-cast steel, but the rate of corrosion declines in the bearing of inhibitor. The activation energy (E_a) was measured by the Arrhenius diagram, achieved by plotting $ln\upsilon_{corr}$ versus 1000/T is presented in **Figure 5**. The transition state and Arrhenius formula are provided:

$$\log(\upsilon_{corr}) = \frac{-E_a}{2.303RT}\ logA$$

$$\upsilon_{corr} = \frac{RT}{Nh}\, e^{\frac{\Delta S^*}{RT}} e^{\frac{\Delta H^*}{RT}}$$

where υ_{corr} is rate of corrosion, A is the pre-exponential factor, R is gas constant, T is temperature, h is Planck's constant, N is Avogadro number, E_a is the activation energy,

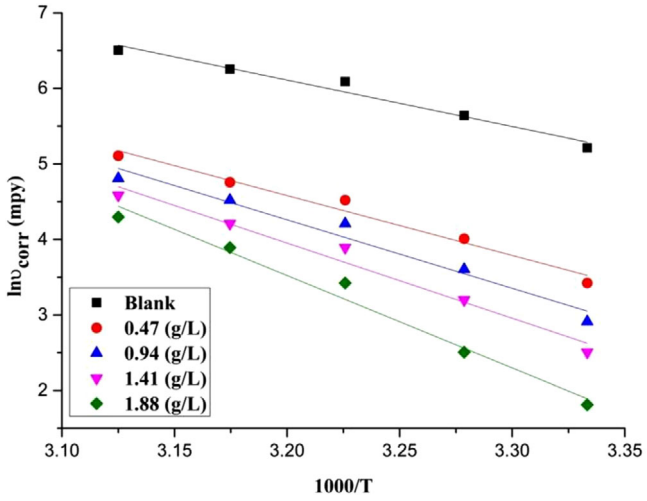


FIGURE 5 Arrhenius plots for soft-cast steel in 1 M HCl solution without and with varying amounts of *CRLE*

ΔS^* is the entropy of activation, and ΔH^* is activation enthalpy. Table 5 lists the measured E_a, A, ΔH^*, and ΔS^* values. As seen in Table 5, the E_a and A results with *CRLE* are predicted to be greater than those without, signifying that the dissolution of soft-cast steel is reduced in the existence of an inhibitor, leading to decreased corrosion rate resulting in the process of forming a protective layer on the surface of soft-cast steel.[28] The values ΔH^* and ΔS^* were determined from the slope (-ΔH*/2.303R) and, intercept ([log(*R*/*Nh*) + ΔS^*/(2.303R)] of the transition plots acquired by the plot of $ln\upsilon_{corr}/T$ versus 1000/T) at all temperature analyzed in the existence of various concentrations of *CRLE* as shown in **Figure 6**. The ΔH^* and ΔS^* values are mentioned in Table 5 and were calculated by the formulae.

$$\Delta H^* = -slope \times R$$

$$\Delta S^* = intercept - ln\left(\frac{R}{Nh}\right)$$

The rise in ΔH^* suggests an endothermic reaction, implying that soft-cast steel dissolution is sluggish, perhaps due to the forming of an energy barrier.[29] The greater ΔH^* value shows that inhibitor molecule adsorption on the soft-cast steel surface is a quasi-substitution mechanism among *CRLE* in the aqueous phase and molecules of H_2O on the soft-cast steel surface.[30] During the rate-determining process, the addition of the inhibitor improves activation of entropy (ΔS^*) values, causing a reduction in disorder from the activated system to the reactants.[31]

Full article
doi.org/10.1002/elsa.202100059
Chemistry Europe
European Chemical Societies Publishing

TABLE 4 The impact of temperature on the $\%\eta_w$ of soft-cast steel in 1 M HCl at various *CRLE* concentrations with a 1-hour immersion time

1 M HCl					
Temp. (in K)	**Concentration (g/L)**	**mass-loss in (mg)**	**Corrosion rate (mpy)**	**Inhibition efficiency ($\%\eta_w$)**	**θ**
300	Blank	30	183.85		
	0.47	5	30.64	83.33	0.8333
	0.94	3	18.38	90	0.90
	1.41	2	12.25	93.33	0.9333
	1.88	1	6.12	96.66	0.9666
305	Blank	46	281.90		
	0.47	9	55.15	82.60	0.8260
	0.94	6	36.77	86.95	0.8695
	1.41	4	24.51	91.30	0.9130
	1.88	2	12.25	95.65	0.9565
310	Blank	72	441.24		
	0.47	15	91.92	79.16	0.7916
	0.94	11	67.41	84.72	0.8472
	1.41	8	49.02	88.88	0.8888
	1.88	5	30.64	93.05	0.9305
315	Blank	85	520.91		
	0.47	19	116.44	77.64	0.7764
	0.94	15	91.92	82.35	0.8235
	1.41	11	67.41	87.05	0.8705
	1.88	8	49.02	90.58	0.9058
320	Blank	109	667.99		
	0.47	27	165.46	75.22	0.7522
	0.94	20	122.56	81.65	0.8165
	1.41	16	98.05	85.32	0.8532
	1.88	12	73.54	88.99	0.8899

TABLE 5 Activation parameters

1 M HCl	**C (g/L)**	**Ea*(kJ/mol)**	**A(kJ/mol)**	**ΔH*(kJ/mol)**	**ΔS*(J mol^{-1} K^{-1})**
	Blank	51.145	1.59451×10^{11}	116.31	-23.69
	0.47	65.949	1.03189×10^{13}	177.33	-23.67
	0.94	75.469	2.92066×10^{14}	211.34	-23.66
	1.41	82.797	3.60104×10^{15}	237.69	-23.65
	1.88	101.752	3.45378×10^{18}	302.96	-23.63

3.5 | Adsorption isotherm and thermodynamic calculations

Corroding surface adsorption cannot reach the equilibrium state and is usually in a stable-state of adsorption. But the rate of corrosion is much strong; the equilibrium state of adsorption continues to be a quasi-static process. In this particular instance, the thermodynamic consideration of quasi-equilibrium adsorption using appropriate equilibrium isotherms is reasonable.[32] As an effective corrosion inhibitor, the efficiency of the *CRLE* mostly relies on the proficiency to adsorb on the metal surface. Therefore the understanding mode of adsorption is necessary, and this will provide fruitful facts regarding the correlation of the

Full article
doi.org/10.1002/elsa.202100059
Chemistry Europe
European Chemical Societies Publishing

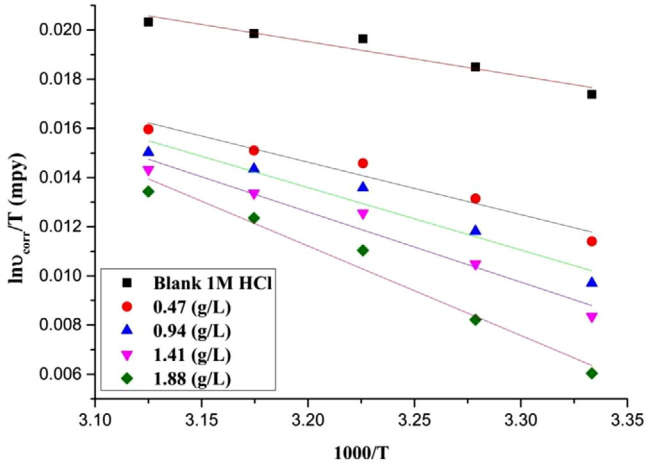


FIGURE 6 Transition state plots for soft-cast steel in 1 M HCl solution with varying amounts of *CRLE* in the absence and presence of *CRLE*

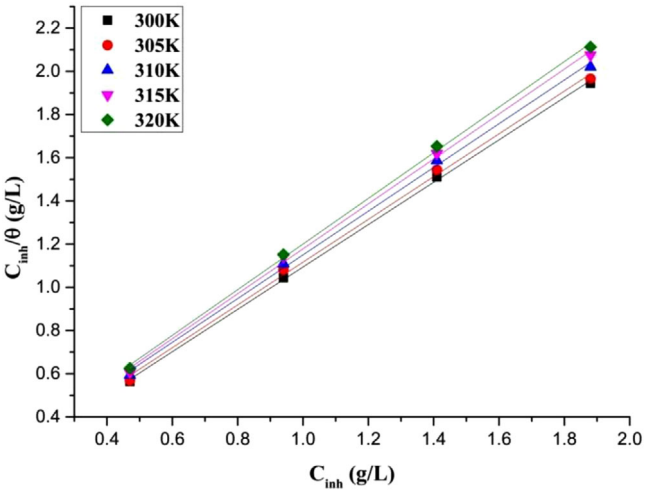


FIGURE 7 Langmuir adsorption isotherms for soft-cast steel in 1 M HCl at varying inhibitor concentrations

inhibitor with the surface of the metal. Many isotherm models have been tried to match experimental results, including Langmuir, Temkin, Freundlich, Frumkin, and, Flory-Huggins to get more details regarding adsorption of *CRLE* on soft-cast steel in 1 M HCl at 300 ± 1 K. The optimal match was obtained using Langmuir's isotherm, which is in remarkable agreement with the following formula.

$$\frac{C}{\theta} = \frac{1}{K_{ads}} + C,$$

where θ is a surface covering, C is the inhibitor concentration described as $\eta_z/100$ at various inhibitor concentrations measured from the mass-loss measurements, and K_{ads} is the equilibrium constant of the binding mechanism associated to ΔG^o_{ads} as follows

$$K_{ads} = \frac{1}{55.5} e^{-\frac{\Delta G^o_{ads}}{RT}}$$

where R is gas constant, T is the absolute temperature, and the molar water concentration is 55.5. The graph of C_{inh}/θ against C_{inh} are presented in Figure 7 are almost straight lines with unit slope.

All regression correlations were calculated are actually nearby 1, signifying Langmuir isotherm can comply with the binding of *CRLE* on the soft-cast steel surface. The inhibitor adsorption on the metal surface is usually assumed to be the crucial move in the inhibition process. It is essential to establish isotherm models, which define the adsorption mechanism of corrosion inhibitors as they provide valuable details regarding the mode of interaction among metal inhibitors.

The adsorbed *CRLE* on soft-cast steel is indicated by the negative values of ΔG^o_{ads}. Physisorption is the electrostatic association between charged particles and the metal's charged surface, and this is typically associated with $-\Delta G^o_{ads}$ values of about or less than -20 kJ/mol. The results around or higher than -40 kJ/mol state that the molecules are corresponding to chemisorption exchange of mean charge or shift of inhibitor to the metal surface to form a co-ordinate type of metal bond.[33]

Table 6 presents the data of K_{ads}, ΔG^o_{ads}, ΔH^o_{ads}, and ΔS^o_{ads}. The values obtained were in the range of -32 to - 34 kJ/mol in the existing research, which states that the adsorption of inhibitor on soft-cast steel is primarily chemisorption. Moreover, free energy adsorption ΔG^o_{ads} values relatively near to -40 kJ/mol suggest that chemisorption imparts substantial participation while physisorption imparts the slightest contribution to the *CRLE* inhibition process.[34] The adsorption enthalpy was inferred by Gibbs Helmholtz formulae

$$\left\{\partial\left(\Delta G^o_{ads}/T\right)/\partial T\right\} p = \frac{-\Delta H^o_{ads}}{T^2}$$

The following equation can be rearranged to give this formula

$$\Delta S^o_{ads} = \frac{\left(\Delta H^o_{ads} - \Delta G^o_{ads}\right)}{T},$$

The graph for $\Delta G^o_{ads}/T$ versus 1000/T is linear as presented in Figure 8 with a slope equivalent to ΔH^o_{ads}, and the intercept is ΔS^o_{ads}. The adsorption enthalpy ΔH^o_{ads} is -9.01 kJ/mol, and adsorption randomness for ΔS^o_{ads} ranges around 78 J/mol/K, accordingly.[35] In this analysis, the ΔH^o_{ads} value is -9.01 kJ/mol, suggesting that *CRLE* adsorption on soft-cast steel surface is an exothermic process with a mostly chemisorption approach.[36] In the presence

Full article
doi.org/10.1002/elsa.202100059
Chemistry Europe
European Chemical Societies Publishing

TABLE 6 Thermodynamic parameters for inhibitor adsorption in 1 M HCl in soft-cast steel at varying temperatures

1 M HCl	Temperature	K_{ads} (L/g)	ΔG^0_{ads}(kJ/mol)	ΔH^0_{ads}(kJ/mol)	ΔS^0_{ads}(J mol^{-1} K^{-1})
	300	8790.43	-32.674	-9.01	78.88
	305	7886.43	-32.943	-9.01	78.47
	310	7231.18	-33.260	-9.01	78.23
	315	7228.56	-33.795	-9.01	78.68
	320	6936.73	-34.222	-9.01	78.79

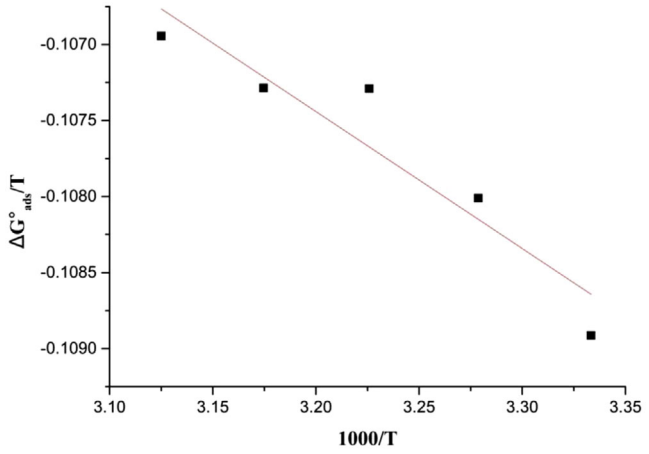


FIGURE 8 Relationship between $\Delta G^o_{ads}/T$ versus 1000/T for 1 M HCl

of *CRLE*, the ΔS^o_{ads} values are high, and negative values suggest a decrease in entropy leading to a decline in disordering as the reactants transition to the steel adsorbed material.[37] The findings of the thermodynamic analysis show the *CRLE* adsorption is systematic chemical adsorption.

3.6 | FT-IR studies

The FT-IR studies of the crude *CRLE* as shown in Figure 9A show broadband observed at 3419 cm^{-1} corresponds to the free –OH group. The adsorption peaks found at 2922 and 2854 cm^{-1} show the presence of –C-H and = C-H stretching. The sharp band at 1663 cm^{-1} is due to the presence of the –C = O group. Similarly –C-O stretching peak is observed at 1344 cm^{-1}. 1015 cm^{-1} and 1088 cm^{-1} are due to the appearance of C-H bending.

The FT-IR spectrum of the specimen upon reaction with an inhibitor-containing acid medium as shown in Figure 9B shows a slight deviation in the peaks compared to that of crude *CRLE*. The broadband at 3447 cm^{-1} confirms the free –OH group. Sharp peaks at 2923 and 2853 cm^{-1} represent the presence of –C-H stretching. Carbonyl group stretching frequency is noticed at 1647 cm^{-1} and band at 1019 cm^{-1} confirms C-H bending vibration.

3.7 | SEM analysis

The scanning electron microscope is utilized to examine the surface morphologies of soft-cast steel in 1 M HCl. The SEM examines the changeover in the morphological features of the soft-cast steel without and with inhibitor.[38] Figure 10A depicts the SEM image of a polished soft-cast steel surface which displays a smooth and clean surface. SEM images for soft-cast steel dipped in 1 M HCl for 2 h immersion time without and with an inhibitor of optimized concentrations of *CRLE* are shown in Figure 10B, 10C, accordingly. The *CRLE* protects the soft-cast steel corrosion on the inclusion of 1.88 g/L of the inhibitor to the corrosive medium, while a great degree of decomposition would be seen on the soft-cast steel surface that had been subjected to corrosive media.

3.8 | AFM study

AFM is a useful aspect for nano-to-microscale investigation of the surface morphology and to evaluate the inhibitor effect on the development and production of corrosion at both metal/solution interfaces. The AFM testing provides the soft-cast steel surface average roughness (R_a), which is helpful in the detection of the inhibitor efficiency. The adsorption mechanism of the *CRLE* on soft-cast steel can be described based on R_a values.[39,40]

In the presence and absence of a *CRLE* inhibitor, the 3D photographs and topography profiles of soft-cast steel are shown in Figure 11 and Table 7. The roughness values obtained represent the mechanism of inhibitor adsorption on soft-cast steel. The polished soft-cast steel surface is shown in Figure 11A, the R_a value is 14.382 nm. The soft-cast steel dipped in 1 M HCl without inhibitor for 2 hours is shown in Figure 11B and has R_a 217.19 nm. But when the soft-cast steel is immersed in 1 M HCl with a 1.88 g/L *CRLE* inhibitor presented in Figure 11C, the R_a value was

Full article
doi.org/10.1002/elsa.202100059
Chemistry Europe
European Chemical Societies Publishing

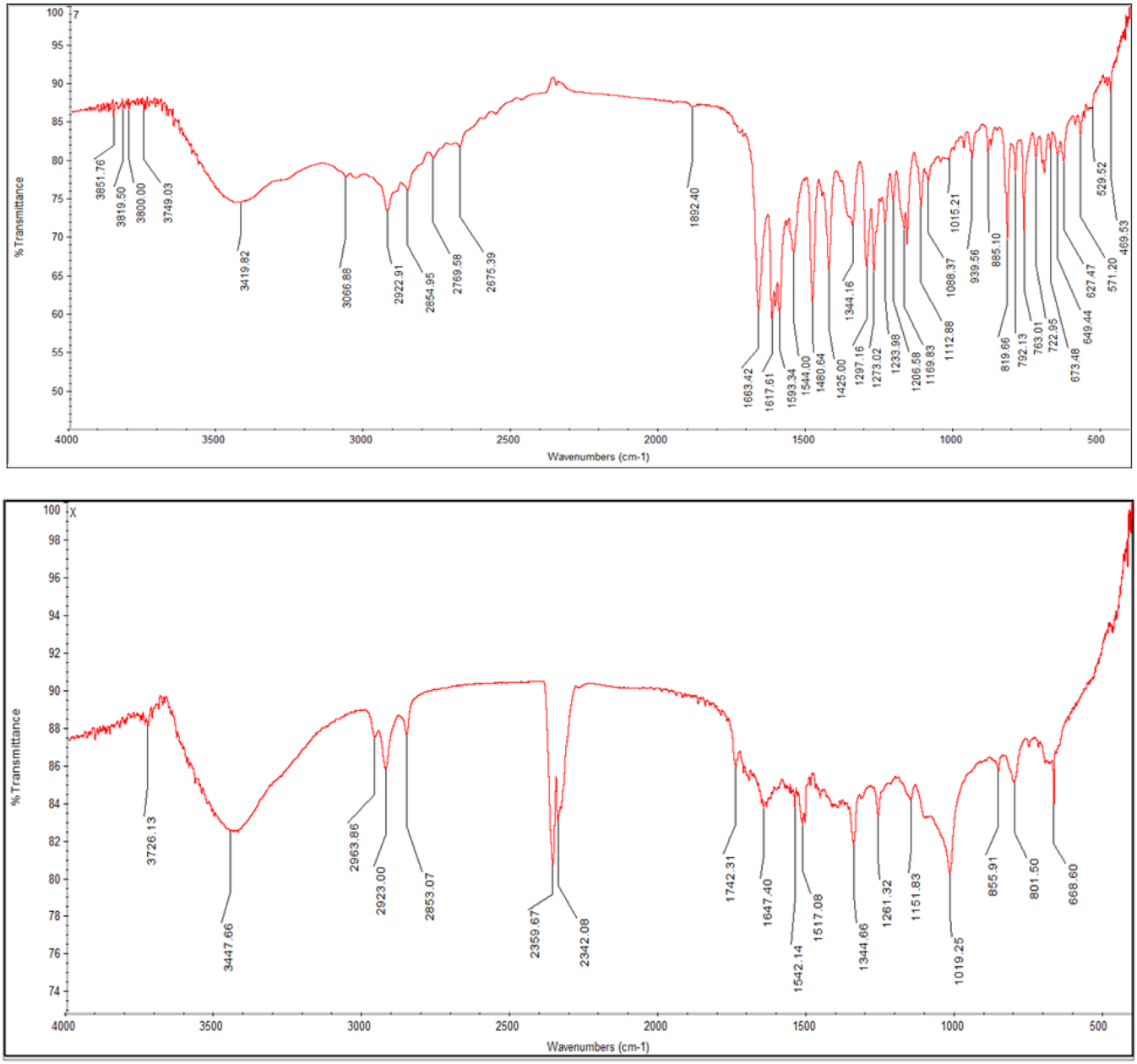


FIGURE 9 The FT-IR spectra of *CRLE*: A = *Cycas revoluta leaves* extract spectrum; B = Scratched compound from the surface of soft-cast steel with *CRLE*FT-IR spectrum

reported to be 88.421 nm, which is less than the default (blank) value. In the existence of inhibitor, a drop in R_a value suggests the binding of inhibitor molecules on a soft-cast steel surface.

3.9 | Contact angle study

The hydrophobicity of the protective coating on the soft-cast steel was measured using the water contact angle.[41] A contact angle investigation is conducted to examine the surface morphologies of soft-cast steel dipped in 1 M HCl without and, with *CRLE*. Table 8 shows the shift of contact angle from the bare to the inhibited specimen. The contact angle of soft-cast steel in 1 M HCl without inhibitor for two hours is 57.2° as seen, in Figure 12A. This is attributed to the unavailability of *CRLE*, the water molecules have more affinity towards the metal surface (more hydrophilic nature). Figure 12B shows a hike in the contact angle to 88.3° that denotes the *CRLE* molecules adsorb on the soft-cast steel in 1 M HCl and actively prevent the dissolution process. This means that there is a decrease in the affinity of water molecules towards the metal surface (reduced in hydrophilic nature) and has decreased wettability due

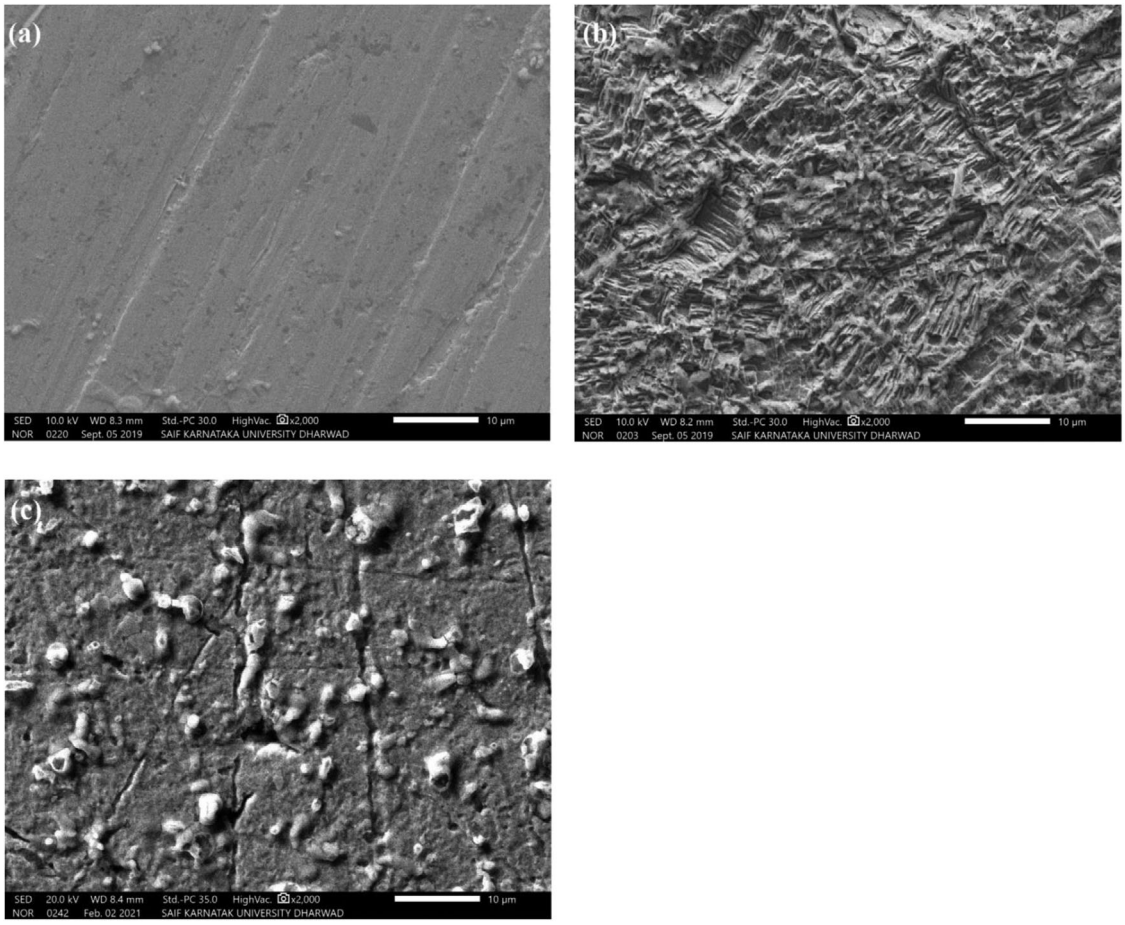


FIGURE 10 Scanning electron micrographic images of soft-cast steel: A = Polished soft-cast steel surface; B = Soft-cast steel in 1 M HCl without inhibitor for 2 h; C = Soft-cast steel dipped for 2 h immersion period in 1 M HCl containing 1.88 (g/L) of the *CRLE*

TABLE 7 AFM results of CRLE

Specimen	Concentration (g/L)	Mean (*Sm*) (fm)	Valley depth (*Sv*)(nm)	Peak height (*Sp*)(nm)	Peak valley height (*Sy*)(nm)	Average roughness (Sa)(nm)	Root mean squareroughness (Sq)(nm)
Polished soft-cast steel	–	-5.744	-82.385	106.09	188.48	14.382	17.966
Blank 1 M HCl	–	-4.647	-928.92	1013.8	1942.7	217.19	270.62
Inhibitor	1.88	-5.744	-441.52	436	877.52	88.421	123.97

to the rise in, hydrophobic nature which indicates the formation of a protective film over the soft-cast steel by active molecules present in *CRLE. D*ue to this, there is a decline in hydrophilicity that avoids corrosion progression.

4 | SUMMARY AND CONCLUSIONS

In 1 M HCl, *CRLE* is a potent inhibitor for corrosion of soft-cast steel, where the inhibition efficiency rises as the inhibitor concentration increases upto1.88 g/L.

- The inhibitor concentration and temperature of the experimental solution usually regulate the inhibition efficiency (η_w) of *CRLE* on the surface of soft-cast steel.
- At an optimized concentration of 1.88 (g/L), the highest η_w of 96.66 was reported for mass-loss in 1 M HCl.
- We can deduce from polarization curves that *CRLE* is a mixed kind of inhibitor.
- Electrochemical impedance calculations (EIS) demonstrate as the inhibitor concentration on the surface of soft-cast steel rises, the (R_p) values rise while the (C_{dl}) values fall, assisting *CRLE* adsorption.

Full article
doi.org/10.1002/elsa.202100059
Chemistry Europe
European Chemical Societies Publishing

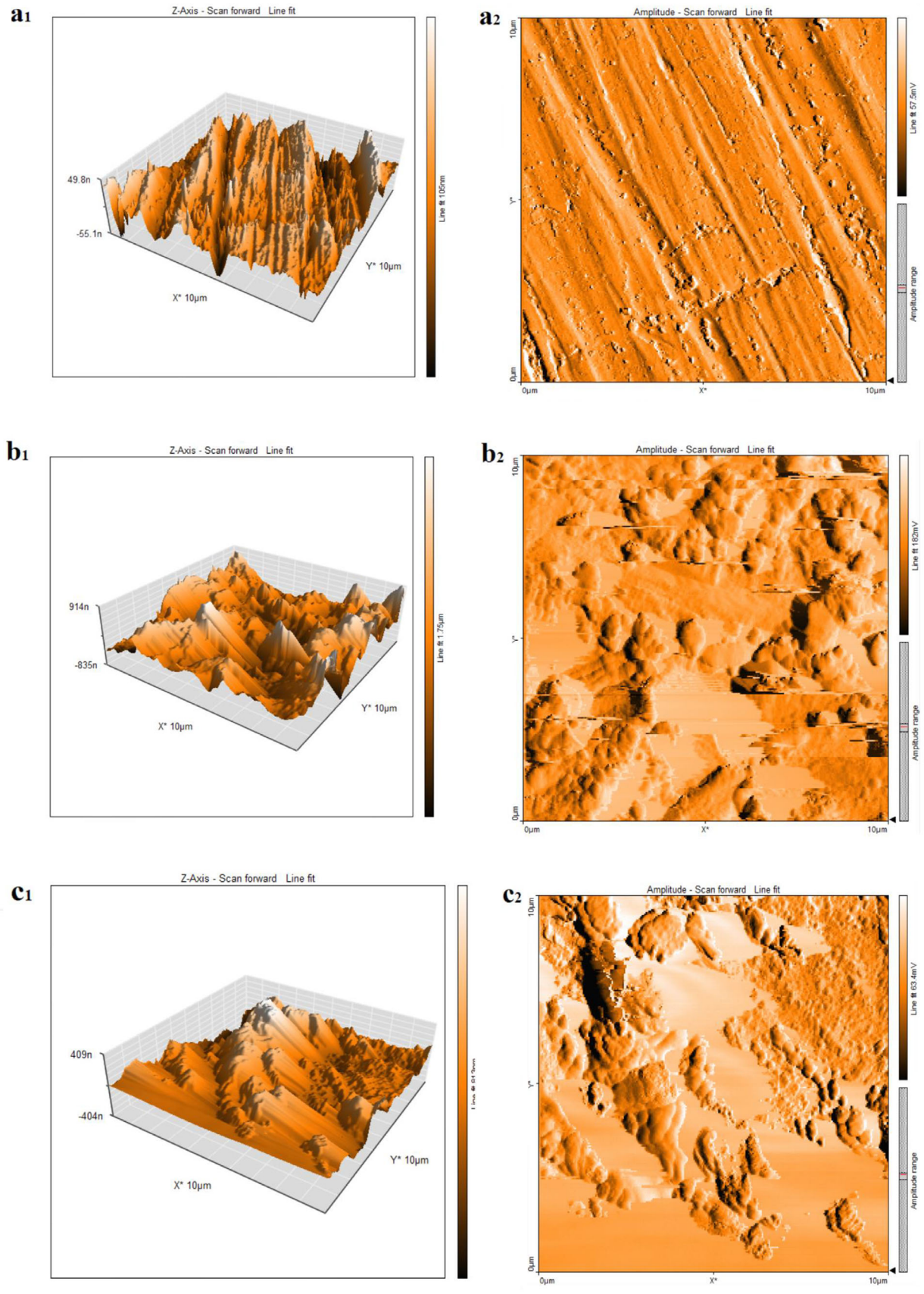


FIGURE 11 The 3D AFM micrographs: A = Polished soft-cast steel surface. B = Soft-cast steel in 1 M HCl without inhibitor for 2 h. C = Soft-cast steel dipped in 2 h immersion period in 1 M HCl containing 1.88 (g/L) of the *CRLE*

Full article
doi.org/10.1002/elsa.202100059
Chemistry Europe
European Chemical Societies Publishing

TABLE 8 Contact angle on soft-cast steel surface

Trial Number	Contact angle (°) Blank	Contact angle (°) 1.88 g /L of *CRLE*
1	57.2	85.9
2	59.3	87.4
3	67.4	88.3
4	68.3	90.3
5	68.8	92.2

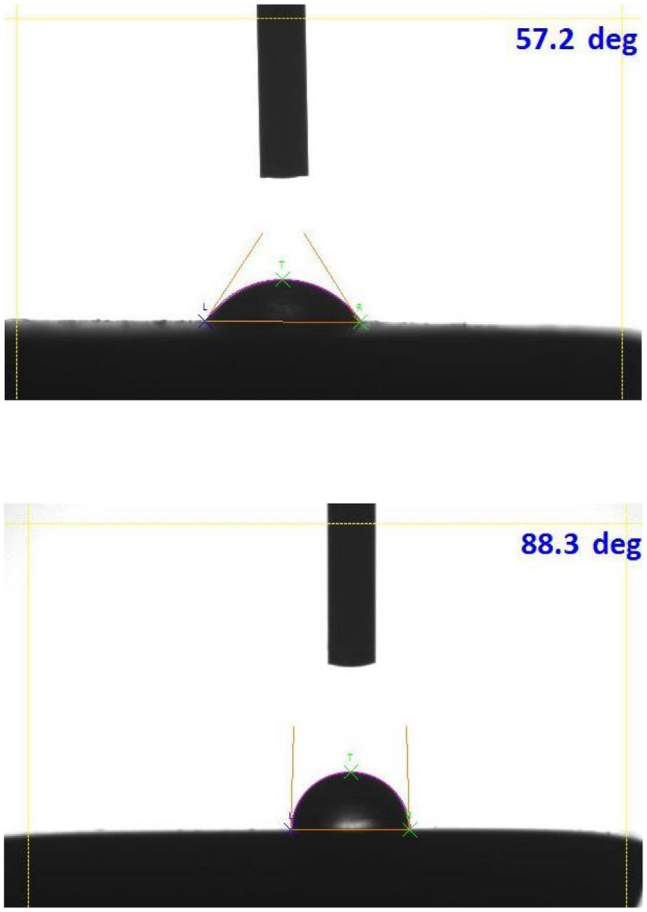


FIGURE 12 Contact tests: A = Soft-cast steel immersed in 1 M HCl (contact angle = 57.2°); B = Soft-cast steel immersed in 1 M HCl with 1.88 g/L of *CRLE* (contact angle = 88.3°)

- The adsorption of *CRLE* from HCl solution on the soft-cast steel surface fulfilled Langmuir's adsorption isotherm.
- Chemisorption is mainly responsible for the inhibitor's adsorption on the soft-cast steel surface.
- Because of the presence of *CRLE,* the corrosion product for soft-cast steel surface is IR active.
- Scanning electron micrographs reveal the inhibitory effects of *CRLE* against corrosion.
- The influence of inhibitor on the surface of soft-cast steel via the adsorption mechanism is supported by AFM and contact angle tests.

ACKNOWLEDGMENTS

The authors of Karnatak Science College, Dharwad thanks the University Sophisticated Instrument Center, and DST-SAIF KUD for FT-IR, SEM, AFM and contact angle studies. One of the authors, Mr. Manohar Rathod is grateful to Karnatak University and Karnatak Science College, Dharwad for University Research Studentship.

DATA AVAILABILITY STATEMENT

The data that support the findings of this study are available on request from the corresponding author.

ORCID

Manohar R. Rathod https://orcid.org/0000-0003-3944-0487
S. K. Rajappa https://orcid.org/0000-0002-8455-4881

REFERENCES

1. G. T. Galo, Morandim-Giannetti, A. d., F. Cotting, I. V. Aoki, I. P. Aquino, *Met. Mater. Int.* **2020**, https://doi.org/10.1007/s12540-020-00679-9.
2. A. G. Kalkhambkar, S. K. Rajappa, G. Janakunavar, K. Sujata, *J. Mater. Environ. Sci.* **2020**, *11*(10), 1626.
3. J. Haque, C. Verma, V. Srivastava, M. A. Quraishi, E. E. Ebenso, *Results Phys.* **2018**, *9*, 1481–1493.
4. P. Singh, E. E. Ebenso, L. O. Olasunkanmi, I. Obot, M. Quraishi, *J. Phys. Chem. C.* **2016**, *120*(6), 3408–3419.
5. M. Faustin, A. Maciuk, P. Salvin, C. Roos, M. Lebrini, *Corros. Sci.* **2015**, *92*, 287–300.
6. H. M. A. El-Lateef, *Corros. Sci.* **2015**, *92*, 104.
7. K. Hu, J. Zhuang, J. Ding, Z. Ma, F. Wang, X. Zeng, *Corros. Sci.* **2017**, *125*, 68.
8. J. K. Wessel, *The Handbook of Advanced Materials: Enabling New Designs* (Wiley, Hoboken, **2004**)
9. A. K. Singh, S. K. Shukla, M. Singh, M. A. Quraishi, *Mater. Chem. Phys.* **2011**, *129*, 68.
10. S. K. Shukla, M. A. Quraishi, *Mater. Chem. Phys.* **2010**, *120*, 142.
11. S. K. Shukla, A. K. Singh, I. Ahamad, M. A. Quraishi, *Mater. Lett.* **2009**, *63*, 819.
12. S. K. Shukla, M. A. Quraishi, *Corros. Sci.* **2009**, *51*, 1007.
13. S. K. Shukla, M. A. Quraishi, R. Prakash, *Corros. Sci.* **2008**, *50*, 2867.
14. Ranney, M. W. *Inhibitors-Manufacture and Technology*; Noyes Data Corp: NJ, **1976**.
15. P. Mourya, S. Banerjee, M.M. Singh, *Corros. Sci.* **2014**, *85*, 352.
16. K. K. Anupama, K. Ramya, K. M. Shainy, A. Joseph, *Mater. Chem. Phys.* **2015**, *167*, 28.
17. E. E. Oguzie, *Corros. Sci.* **2008**, *50*, 2993.
18. A. K. Satapathy, G. Gunasekaran, S. C. Sahoo, K. Amit, P. V. Rodrigues, *Corros. Sci.* **2009**, *51*, 2848.
19. A. Moawad, M. Hetta, J. Zjawiony, M. Jacob, M. Hifnawy, J. Marais, & D. Ferreira, *Planta Medica.* **2010**, *76*(08), 796.

20. G. S. Deora, K. Monika, S. Sarswati, *Pharmacogn J.* **2020**, *12*(5), 1165.
21. M. K. Mourya, A. Prakash, A. Swami, G. K. Singh and A. mathur, *World j. sci. technol.* **2011**, *1*(10), 11.
22. S. Merah, L. Larabi, O. Benali, Y. Harek, *Pigm Resin Technol.* **2008**, *37*, 291.
23. S. A. Ali, A. M. El-Shareef, R. F. Al-Ghandi, M. T. Saeed, *Corros. Sci.* **2005**, *47*, 2659.
24. D. Jayaperumal, *Mater. Chem. Phys.* **2010**, *119*, 478.
25. F. Bentiss, M. Lebrini, H. Vezin, F. Chai, M. Traisnel, M. Lagrenee, *Corros. Sci.* **2009**, *51*, 2165.
26. B. M. Prasanna, B. M. Praveen, N. Hebbar, T. V. Venkatesha, H.C. Tandon, *Ind. Eng. Chem. Res.* **2014**, *53*, 8436.
27. D. Thirumoolan, V. A. Katkar, G. Gunasekaran, T. Kanai, K.A. Basha, *Prog. Org. Coat.* **2014**, *77*, 1253.
28. A. S. Fouda, M. Eissa, A. El-Hossiany, *Int. J. Electrochem. Sci.* **2018**, *13*, 11096.
29. A. M. Guruprasad, H. P. Sachin, G. A. Swetha, B. M. Prasanna, *Int. J. Ind. Chem.* **2019**, *10*, 17.
30. P. Singh, V. Srivastava, M. A. Quraishi, *J. Mol. Liq.* **2016**, *216*, 164.
31. A. Dandia, S. L. Gupta, P. Singh, M. A. Quraishi, *Chem. Eng.* **2013**, *1*, 1303.
32. C. B. Pradeep Kumar, K. N. Mohana, *Int. Res. J. Pure Appl. Chem.* **2013**, *3*, 330.
33. A. K. Singh, *Ind. Eng. Chem. Res.* **2012**, *51*, 3215.
34. T. Poornima, J. Nayak, N. A. Shetty, *J. Appl. Electrochem.* **2011**, *41*, 223.
35. M. K. Pavithra, T. V. Venkatesha, M. K. Punith Kumar, H. C. Tondan, *Corr. Sci.* **2012**, *60*, 104.
36. I. B. Obot, N. O. Obi-Egbedi, A. O. Eseola, *Ind. Eng. Chem. Res.* **2011**, *50*, 2098.
37. G. E. Badr, *Corros. Sci.* **2009**, *51*, 2529.
38. N. Raghavendra, J. I. Bhat, *Chem. Eng. Commun.* **2018**, *205*(2), 145.
39. E. A. F. S. Abd, A. H. Ali, *Zast. Mater.* **2018**, *59*, 126.
40. A. S. Fouda, G. El-Ewady, A. H. Ali, *J. Appl. Chem.* **2017**, *6*, 701.
41. N. Raghavendra, L. V. Hublikar, S. M. Patil, P. J. Ganiger, A. S. Bhinge, *Bull. Mater. Sci.* **2019**, *42*(5), 226.

How to cite this article: M. R. Rathod, S. K. Rajappa, *Electrochem Sci Adv*. **2022**, *2,* e2100059. https://doi.org/10.1002/elsa.202100059